THE JOURNAL OF PHYSICAL CHEMISTRY C

ARTICLE

pubs.acs.org/JPCC

Controlled Growth of Multilayer, Few-Layer, and Single-Layer Graphene on Metal Substrates

Yagang Yao,[†] Zhuo Li,[†] Ziyin Lin,[†,‡] Kyoung-Sik Moon,[†] Josh Agar,[†] and Chingping Wong*[,†,§]

[†]School of Materials Science and Engineering, Georgia Institute of Technology, 771 Ferst Drive NW, Atlanta, Georgia 30332, United States

[‡]School of Chemistry and Biochemistry, Georgia Institute of Technology, 901 Atlantic Drive NW, Atlanta, Georgia 30332, United States

[§]Faculty of Engineering, The Chinese University of Hong Kong, Shatin, Hong Kong, China

ABSTRACT: The effects of graphene growth parameters on the number of its layers were systematically studied and a new growth mechanism on Cu substrate was thus proposed. Through the investigation of the graphene growth parameters, including growth substrate types, carrier gases, types of carbon sources, growth temperature, growth time, and cooling rates, we found that graphene grows on Cu substrates via a surface-catalyzed process, followed by a templated growth. We can obtain either single layer graphene (SLG) or few-layer graphene (FLG) by suppressing the subsequent templated growth with a low concentration of carbon source gases and a high concentration of H_2. Our findings provide important guidance toward the synthesis of large-scale and high-quality FLGs and SLGs. This is expected to widen both the research and applications of graphene.

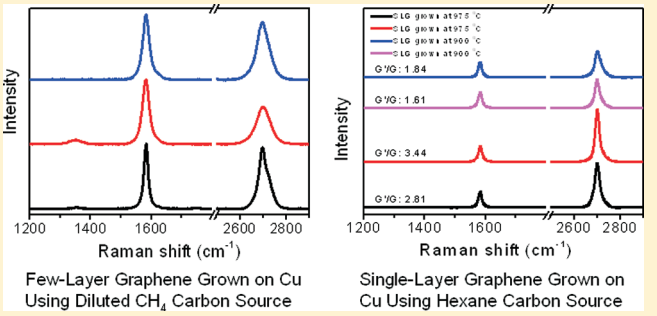

1. INTRODUCTION

Graphene, a single layer of sp^2 carbon atoms bonded in a hexagonal lattice, has many extraordinary properties, such as large specific surface area,[1] large Young's modulus,[2] high charge carrier mobility,[3] and thermal conductivity.[4] Such unique properties make graphene a promising candidate for widespread applications in post-silicon electronics,[5−8] sensors,[9−12] and energy storage devices.[1,13,14] However, the properties of graphene heavily depend on the number of layers. Ghosh et al. have shown that the room temperature thermal conductivity of graphene changes from ∼2800 to ∼1300 W m^{-1} K^{-1} as the number of atomic planes in a few-layer graphene (FLG) increases from 2 to 4.[15] Nair et al. demonstrated that the single-layer graphene (SLG) absorbs $\pi\alpha \approx$ 2.3% of white light while the adsorption of FLG is equal to 2.3% multiplied by the number of layers.[16] Therefore, different applications will have specific requirements for the layer number of graphene. In order to make full use of graphene's unique properties in each application, it is crucial to control the number of layers.

In addition to the layer control, large-scale production capability for high-quality graphene is another important requirement for its real-life applications. So far, several techniques have been developed to produce graphene, including micromechanical exfoliation of highly oriented pyrolytic graphite (HOPG),[17,18] ultrasonication exfoliation of graphite,[19,20] chemical reduction of graphite oxide (GO),[21−24] carbon nanotube (CNT) unzipping,[25,26] and epitaxial and chemical vapor deposition (CVD) growth.[27−39] Among these methods, chemical reduction of GO, epitaxial growth, and CVD growth may have the potential for industrial production. However, for the chemical reduction method, it is very challenging to recover the seriously defected GO to pristine graphene. Thus, the exotic properties of graphene such as the high charge carrier mobility and optical properties are hard to achieve.[40,41] Epitaxial growth is a promising route to produce high-quality graphene, yet this method requires stringent and costly growth conditions such as high growth temperature (usually higher than 1000 °C), high vacuum, and expensive substrate materials. The most promising method for mass production of high-quality graphene could be the CVD method. Nowadays, CNTs from CVD growth occupy the majority of the commercially available CNTs. We expect a similar phenomenon to appear for the graphene market in the near future. In 2009, Kong's team first discovered that FLG could be grown on a 300 nm Ni film.[28] The catalyst was e-beam evaporated onto SiO_2/Si substrates and thermally annealed prior to the atmospheric pressure CVD synthesis. The as-produced graphene can be transferred to nonspecific substrate using poly(methyl methacrylate) (PMMA)-mediated nanotransfer printing.[42,43] Almost at the same time, Kim et al. also reported FLG growth in atmospheric pressure CVD by using an e-beam deposited Ni film.[29] The authors used poly(dimethylsiloxane) (PDMS) to transfer the as-grown graphene and showed that graphene could be used as stretchable transparent electrodes. In the same year, Chae et al. reported the large-area multilayer graphene (MLG) synthesis on a nickel foil substrate by CVD.[31] Des-

Received: September 20, 2010
Revised: November 24, 2010
Published: March 11, 2011

   dx.doi.org/10.1021/jp109002p | *J. Phys. Chem. C* 2011, 115, 5232–5238

pite the high quality of graphene, these methods did not provide an efficient way to control the number of layers. Li et al. has showed that SLG could be grown on copper substrates, but the high vacuum in the growth process leads to a significant cost issue.[34] Few studies on controlling the number of graphene layers have been reported, although the layer number plays an important role in customizing graphene properties. Furthermore, the growth mechanism of graphene to create a favorable environment for SLG growth has not been elucidated.

In this work, we investigated the effects of several growth parameters on the graphene layers in atmospheric pressure CVD and proposed a new growth mechanism of graphene on Cu substrates, that is, a surface-catalyzed process and a subsequent templated growth. The templated growth should be suppressed in order to obtain thinner graphene layers. These findings provide an important route toward the fabrication of large-scale and high-quality FLG and SLG samples. The liquid-precursor-based synthesis step will open up a window not only for SLG growth but also the doped graphene fabrication by using various nitrogen- or boron-containing organic liquid precursors.

2. EXPERIMENTAL DETAILS

2.1. Atmospheric Pressure CVD Synthesis of MLG, FLG, and SLG Films. Fe, Co, and Ni foils (100 μm thick, 99.95% metal basis) and Cu foils (125 μm thick, 99% metal basis) were purchased from Sigma-Aldrich and Basic Copper, respectively, as the growth substrates. These substrates were used as received. Gas precursors ethylene and methane and a liquid precursor hexane were used as carbon sources. The substrates were placed in a tube furnace and heated to a temperature of 975 °C for methane and ethylene and 975 or 900 °C for hexane. An initial annealing of the metal substrate was carried out in flowing of 500 standard cubic centimeters per minute (sccm) H_2 for 20 min at 975 or 800 °C in order to recover a pure metal surface. Then the gas mixture of a carbon source and H_2 was introduced into the furnace with various ratios of a carbon source gas to H_2 (C_2H_4/H_2 = 2.5/200, 5/200, 7.5/200, 10/200, 2.5/500, 5/500, 7.5/500, and 10/500; CH_4/H_2 = 2.5/500, 5/500, and 7.5/500). The growth time was 3 or 5 min for methane and ethylene. The hexane vapor concentration in the CVD chamber was controlled by bubbling a small amount of argon gas through liquid hexane. The growth time was 3 s. After completion of growth, the carbon source supply was stopped, and the furnace was cooled down to room temperature in flowing of 350 sccm Ar and 150 sccm H_2 with a cooling rate of 10 °C min^{-1}, or to 500 °C by fast cooling with a cooling rate of 150 or 600 °C min^{-1}.

2.2. Characterizations. Scanning electron microscopy (SEM, JEOL 1530 and 1550) and optical microscopy were used to observe the morphology and homogeneity of as-produced graphene films. Raman spectroscopy (Jobin Yvon, Aramis) with laser excitation wavelengths of 532 nm was performed throughout the metal substrates after the CVD process to confirm the formation of graphene and characterize the quality and the number of layers of as-produced graphene.

3. RESULTS AND DISCUSSION

3.1. MLG and FLG Growth on Ni, Fe, Co, and Cu Foils by Using Ethylene as the Carbon Source at 975 °C for 3 min. It is well-known that different kinds of metal nanoparticles, like Fe, Co, Ni, Cu, Au, etc., and even nonmetal nanoparticles such as SiO_2, SiC, Ge, and Al_2O_3 can be used as catalysts to grow high-quality CNTs.[44−46] There might be two reasons for the high efficiency growth of CNTs: one is that the solubility of carbon into metal particles at the growth temperature is relatively high, which would provide enough carbon for CNT formation; the other is the high catalytic activity of these particles, which can lower the formation energy of CNT and accelerate the decomposition of the carbon source. Therefore, the catalysts play an important role in CVD growth of CNT. Similar to CNT growth, metal substrates or catalysts are also critical in graphene growth. Typically e-beam deposited Ni and Cu films or Ni and Cu foils were used as the growth substrates. However, it is not clear the role of metal in graphene growth. So we chose different metals including Ni, Fe, Co, and Cu to investigate their effect on graphene synthesis.

Figure 1 shows typical growth and characterization results of MLG and FLG on Ni, Fe, Co, and Cu substrates by using ethylene as the carbon source. Compared to CH_4, which is a commonly used carbon source for graphene growth, C_2H_4 has a lower decomposition temperature. Figure 1a shows a representative optical microscopy image of synthesized graphene on a Ni substrate (1.5 cm × 1.5 cm). Obviously the film is continuous and the grain boundary is clearly observed in the image. The corresponding SEM image in Figure 1b also exhibits good homogeneity. It is clear that the film is composed of many domains with a few μm^2 in area. Within the domains, graphene layers are continuous and do not display any structural features, while others have wrinkles extruding from the domains. Lee et al. proposed that the wrinkles were formed by the nucleation of a defect line on step edges and thermal-stress-induced formation of wrinkles around step edges and defect lines.[31] Compared with the SEM and optical microscopy images in the literature, it is obvious that continuous MLG films were obtained when using Ni foils as the substrate and ethylene as the carbon source. Similar optical microscopy and SEM results are shown in panels d and e and panels g and h of Figure 1 for graphene growth on Fe and Co foil substrates, respectively, also indicating the MLG film growth. When comparing Figure 1b with Figure 1e,h, we found that graphene films grown on Fe and Co foils were rougher than that grown on Ni foil. For the Co foil substrates, more wrinkles are clearly visualized in the SEM image in Figure 1h.

Raman spectroscopy is a powerful tool to characterize carbon materials and allow nondestructive identification of produced graphene. It has been reported that it is useful to evaluate the quality of graphene based on the ratio of high-frequency first-order scattering (i.e., the G-band) to second-order scattering (the D-band).[47] Moreover, it can be used to identify the number of layers in the graphene film. According to the D-band and G′-band change in shape, width, and position, the slight downshift of the G peak for an increasing number of layers (for small layers), and the G to G′ peak intensity ratio ($I_G/I_{G'}$), we can distinguish the number of graphene layers.[28,47,48] We used Raman spectroscopy to measure various locations on the metal substrates after graphene growth using ethylene as the carbon source at 975 °C, and representative results are shown in Figure 1c,f,i for the as-grown graphene on Ni, Fe, and Co foils, respectively. Similar to previous Raman results of CVD grown graphene and mechanically exfoliated graphene,[31] the two most intense Raman peaks are the G peak at ∼1580 cm^{-1} and the G′ peak at ∼2700 cm^{-1}. The G peak denotes the symmetry-allowed graphite band and is due to the doubly degenerate zone center E_{2g} mode; this is observed in all sp^2 carbon materials. The G′ peak is the second order of zone-boundary phonons. According to the shape and position

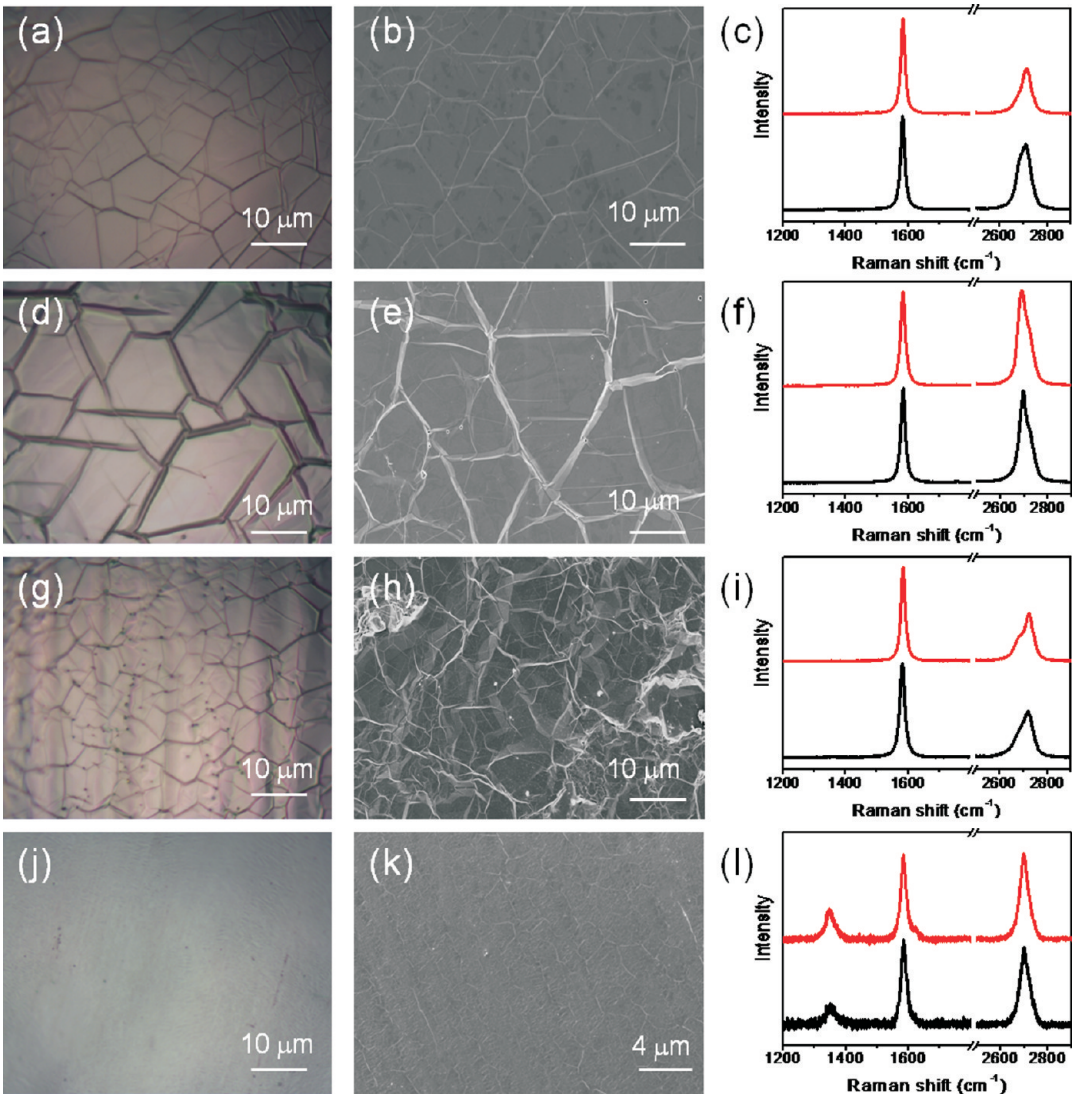

Figure 1. Typical optical microscopy images, SEM images, and Raman spectroscopy of MLG and FLG grown on Ni (a−c), Fe (d−f), Co (g−i), and Cu (j−l) foil substrates using ethylene as the carbon source at 975 °C. The growth time was 3 min, and the gas mixing ratio of C_2H_4/H_2 was 5/500, and the cooling rate was 60 °C min^{-1}. (a, d, g, and j) Optical microscope images of graphene. (b, e, h, and k) SEM images of graphene. (c, f, i, and l) Raman spectroscopy of graphene. Cu substrate background was subtracted. The spectra were normalized with the G-band.

of the G′ peak, the graphene films grown on Ni, Fe, and Co were MLG. This result is consistent with the optical microscopy and SEM characterizations. In addition, it is worth noting that no appreciable disorder-induced D-peak around ∼1350 cm^{-1} was observed in Figure 1c,f,i, indicating the high quality of graphene films grown on Ni, Fe, and Co foils.

While MLG was grown on Ni, Fe, and Co foil substrates, FLG was grown on Cu substrates with using ethylene as the carbon source at 975 °C for 3 min. Typical results of optical microscopy, SEM and Raman spectroscopy characterizations are shown in Figure 1j,k,l. Deduced from the optical microscopy image in Figure 1j, after graphene growth, the Cu substrate image appears to be relatively brighter but slightly speckled. Although the grain size shown after the graphene growth was smaller than that on a blank Cu foil, the as-grown graphene film was still continuous across these visible Cu substrates. The corresponding SEM image in Figure 1k shows homogeneity and continuity of the film. Raman spectra in Figure 1l show small values for the $I_G/I_{G'}$ ratios which is the typical signature of FLG. In addition to the two major G and G′ peaks, a weaker D-band was also observed at ∼1350 cm^{-1} in most of the scanned areas. This peak is due to the disorder or defect in the perfect graphite, such as edges, point defects, and subdomain boundaries, which indicates that the graphene deposited on the Cu substrate has lower quality compared with those grown on Ni, Fe, and Co foils.

According to the above results (continuous FLG growth on Cu foils compared with MLG growth on Ni, Fe, and Co foils), it is desirable to use Cu foils as the growth substrates for FLG and SLG growth. To understand these results, we propose that the solubility of carbon in those metals accounts for the different morphology of graphene on substrates. The order of the carbon solubility in metal is Fe > Co > Ni ≫ Cu.[49,50] We assume that on Ni, Fe, and Co foil substrates, the typical proposed dissolution−precipitation process plays a major role. At the first stage, the carbon source decomposes at a high temperature and the carbon atoms are incorporated into the Ni, Fe, or Co substrates. At the second stage, graphene precipitation is promoted by the out-diffusion of the incorporated carbon on the surface catalyst film

dx.doi.org/10.1021/jp109002p |J. Phys. Chem. C 2011, 115, 5232–5238

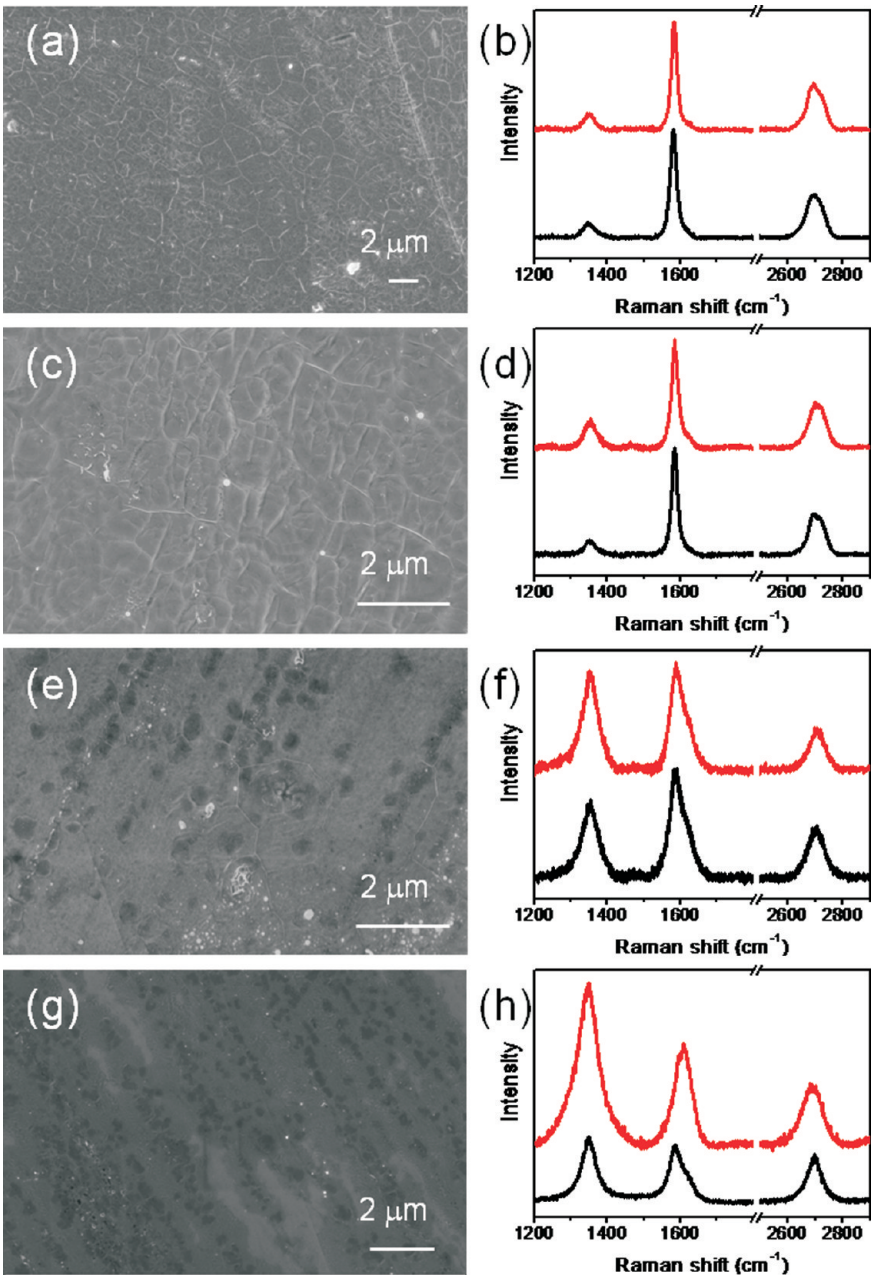

Figure 2. Typical SEM (a, c, e, and g) and Raman spectra (b, d, f, and h) data of graphene films grown on Cu foil substrates at 975 °C using 200 sccm H_2 and various flow rates of C_2H_4 for 5 min. Cu substrate background was subtracted. The spectra were normalized with the G-band. The flow rates of C_2H_4 were 2.5 sccm (a and b), 5 sccm (c and d), 7.5 sccm (e and f), and 10 sccm (g and h).

upon cooling of the substrates.[31] On the basis of the growth process, the growth substrates, growth temperature, growth time, carbon source, carrier gas, and cooling rate are important factors in graphene growth. Kong's group and Yu et al. have demonstrated that graphene segregated from a Ni surface by cooling down with different rates.[27,30] Lee's group reported that the quality of graphene films on Ni foils was greatly improved when the growth temperature was changed from 700 to 975 °C using acetylene as the carbon source.[31] While for Cu foil substrates, the carbon solubility in it is low, so we assume it is a surface-catalyzed process to grow SLG, followed by a templated growth to grow FLG. Ruoff's group has proposed that the growth mechanism of graphene on Cu substrates is not a precipitation process but rather a CVD process.[34] Nicholas et al. have demonstrated the templated growth of extended graphenic sheets by additionally reacting carbon into a preexisting graphene sheet.[51] On the basis of the proposed growth mechanism for Cu substrates, it is possible to control the number of graphene layers by inhibiting the second templated growth stage. Also, graphene synthesis would not be related with the cooling rate. Indeed, when the cooling rate was varied from 10 to 600 °C/min, no obvious differences were observed in the obtained graphene films. To further confirm that carbon solubility in metals determines the graphene growth mechanism, we tried Cr as the substrate, which has much higher solubility of carbon than Ni, Fe, Co, and Cu. We deposited 300 nm thick Cr on Si wafers with thermally oxidized 300 nm SiO_2. The carbon materials grown on Cr at the same condition as discussed above displayed a graphite-like Raman characteristic with a high D band peak.

dx.doi.org/10.1021/jp109002p |*J. Phys. Chem. C* 2011, 115, 5232–5238

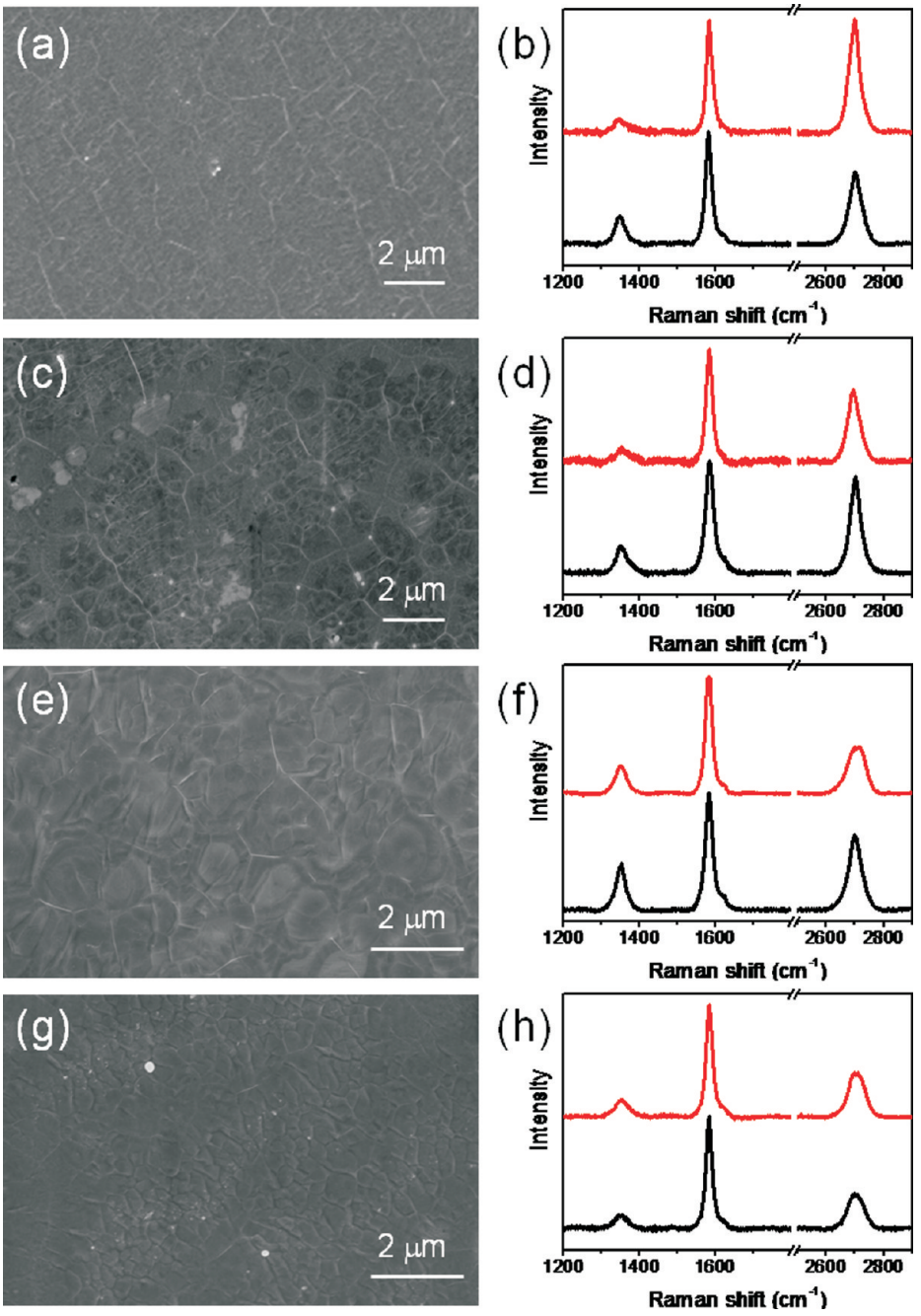

Figure 3. Typical SEM (a, c, e, and g) and Raman spectra (b, d, f, and h) data of graphene films grown on Cu foil substrates at 975 °C by using 500 sccm H_2 and various C_2H_4 for 5 min. Cu substrates background was subtracted. The spectra were normalized with the G-band. The rates of C_2H_4 were 2.5 sccm (a and b), 5 sccm (c and d), 7.5 sccm (e and f), and 10 sccm (g and h).

3.2. Carrier Gas Investigation in Graphene Growth on Cu Foils Using Ethylene as the Carbon Source for Suppressing the Templated Growth. On the basis of the above proposed growth mechanism on Cu substrates, the number of graphene layers can be controlled by suppressing the templated growth. There are several crucial factors to affect the layer number including carrier gas, the concentration of carbon source, types of carbon sources, and growth time. First of all, we investigated the dependence of the number of graphene layers on the concentration of carbon sources and H_2. Figure 2 shows SEM images and corresponding Raman spectra varying the flow rate of C_2H_4 at a fixed 200 sccm of H_2 at the growth temperature of 975 °C for 5 min. At the C_2H_4/H_2 ratios of 2.5/200 and 5/200, good homogeneity and a few domains were observed in Figure 2a,c, respectively. Raman spectra data in Figure 2b,d show two intense G and G′ peaks with typical MLG Raman characteristics on both top and bottom surfaces of the Cu foil and a weaker D band. With increase of the C_2H_4/H_2 ratios to 7.5/200 and 10/200, amorphous carbon like structures were found based on the SEM images shown in Figure 2e,g. Further Raman characterizations in Figure 2f,h show strong D peaks around 1350 cm^{-1}, which confirmed the amorphous morphology of the films made. Therefore, the diluted carbon source is critical for graphene growth and it can inhibit the templated growth at the proposed second stage of graphene formation on Cu substrates.

dx.doi.org/10.1021/jp109002p |J. Phys. Chem. C 2011, 115, 5232–5238

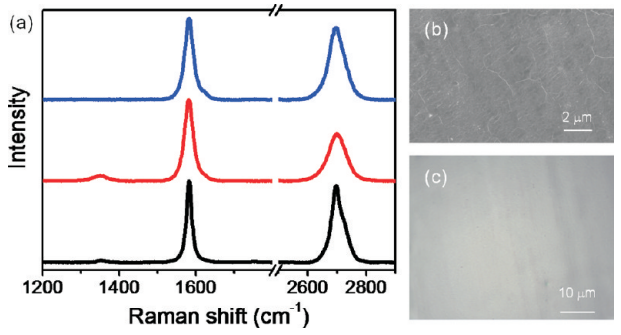

Figure 4. Typical Raman spectroscopy (a), SEM (b), and optical microscopy (c) characterization results of graphene films grown on Cu substrates using CH_4 as the carbon source at the growth temperature of 975 °C for 5 min. For Raman spectra, Cu substrate background was subtracted. The spectra were normalized with the G-band.

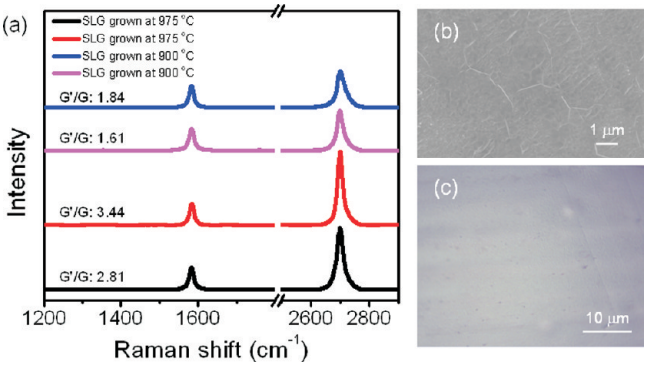

Figure 5. Typical Raman spectroscopy (a), SEM (b), and optical microscopy (c) characterization results of graphene films grown on Cu substrates using hexane as the carbon source at the growth temperature of 975 or 900 °C for 3 s. For Raman spectra, Cu substrate background was subtracted. The spectra were normalized with the G-band.

We also found that H_2 plays an important role in graphene growth. We investigated the H_2 effect on the graphene growth by increasing H_2 flux from 200 to 500 sccm. As shown in Figure 3a,c, at the C_2H_4/H_2 ratios of 2.5/500 and 5/500, continuous films with good homogeneity were obtained. The corresponding Raman spectra data (Figure 3b,d) show two intense G and G′ peaks, a weaker D peak, and small values for the $I_G/I_{G'}$ ratio. This confirmed fewer defects and highly crystalline FLG growth on Cu foil substrates rather than MLG growth at 200 sccm H_2 at the same rate of C_2H_4. At the C_2H_4/H_2 ratios of 7.5/500 and 10/500, instead of amorphous carbon like structures at 200 sccm H_2, uniform graphene films were observed in SEM images (Figure 3e,g, respectively). Raman data in Figure 3f,h show typical MLG Raman characteristics with relatively large values for the $I_G/I_{G'}$ ratio. Compared with the graphene grown at 200 sccm H_2 in Figure 2, the results indicated that introduction of more H_2 gas would be beneficial for suppressing the templated growth. Here, H_2 may help with the etching of carbon, which was also found in CNT synthesis before.[52] Therefore, the amount of H_2 gas determines the number of graphene layers.

3.3. Types of Carbon Source Investigation in Graphene Growth on Cu Foil for Suppressing the Template Growth. On the basis of the above results, C_2H_4 is a not an ideal carbon source for SLG production. Through analyzing the CVD growth process of graphene, we found that the decomposition temperature of carbon sources might be critical for graphene growth. Thus, we chose other carbon sources such as CH_4 and a liquid organic precursor hexane. The decomposition rate is easier to control for CH_4, which has a higher decomposition temperature than that of C_2H_4. Figure 4a shows typical Raman spectra of graphene films at 5 sccm CH_4 as the carbon source and 500 sccm H_2 at the growth temperature of 975 °C for 5 min. A low intensity of D peaks was observed indicating the high quality of graphene films. The small $I_G/I_{G'}$ values provide direct evidence of FLG (two to three layers) synthesis on Cu foil substrates using CH_4 as the carbon source.[28] SEM and optical microscopy images shown in Figure 4b,c, show good homogeneity of the produced graphene films. Moreover, compared with the results of using C_2H_4 as the carbon source, thinner graphene films could be obtained using CH_4 as the carbon source. These results indicated that higher decomposition temperature of hydrocarbon gas would be favorable for suppressing the templated growth on Cu substrates and thus for controlling the number of graphene layers.

Liquid precursors like hexane, benzene, and cyclohexane have been widely used for CNT synthesis because of its availability. Ajayan et al. recently have demonstrated the feasibility of using a liquid hexane precursor as the carbon source for graphene growth.[39] Here we also tried the hexane as a precursor and chose a relatively short growth time (3 s) and high H_2 flux (1000 sccm) to suppress the templated growth. Typical characterization results are shown in Figure 5. Raman data in Figure 5a show a sharp and single Lorentzian G′ peak with a full width at half-maximum of ~27 cm^{-1} and small $I_G/I_{G'}$ ratios which are the signature of SLG. All the scanned areas display hallmarks of SLG, indicating a high percentage of SLG in the graphene film made. This also supported our findings that a diluted carbon source and a high volume of H_2 gas are critical for graphene growth. Moreover, it is worth noting that no visible D band appeared in the grown materials, strongly indicating the high quality graphene formed. More importantly, when the growth temperature was lowered from 975 to 900 °C, high-quality SLGs were still obtained as shown in Figure 5a as pink and blue spectra. Corresponding SEM and optical microscopy results in Figure 5b,c show that the graphene is highly uniform and continuous. When we increased the growth time to 10 and 200 s, Raman spectra (not shown here) suggest that the number of graphene layers increased from SLG to MLG to thicker graphitic layers (>20 layers) and no visible FLG growth was found. Further study is currently underway in order to explore this phenomenon and gain a deeper understanding of this process. The above-mentioned liquid hexane based growth will certainly have great advantages over the typical hydrocarbon gas based growth method.

4. CONCLUSION

In summary, we have proposed a new growth mechanism of graphene on Cu substrates based on the results we got on Ni, Fe, Co, and Cu substrates. It is a surface-catalyzed process to grow SLG, followed by a templated growth to grow FLG. In order to make thinner graphene layers, the templated growth should be suppressed. We found that diluted CH_4 or C_2H_4 and high volume H_2 gas are critical to suppress the templated growth and hence the graphene layer control. Moreover, we found that SLG can be grown on Cu substrates by introducing a small amount of a liquid hexane precursor. However, further study is needed to gain a deeper understanding of this process.

dx.doi.org/10.1021/jp109002p |J. Phys. Chem. C 2011, 115, 5232–5238

The liquid-precursor-based synthesis step will open up a window for doped SLG growth using various nitrogen- or boron-containing organic liquid precursors. Our findings may facilitate both the large-scale synthesis of well-controlled graphene features and a wide range of applications of graphene.

AUTHOR INFORMATION

Corresponding Author

*E-mail: cp.wong@mse.gatech.edu.

REFERENCES

(1) Stoller, M. D.; Park, S. J.; Zhu, Y. W.; An, J. H.; Ruoff, R. S. *Nano Lett.* **2008**, *8*, 3498–3502.

(2) Lee, C.; Wei, X. D.; Kysar, J. W.; Hone, J. *Science* **2008**, *321*, 385–388.

(3) Bolotin, K. I.; Sikes, K. J.; Jiang, Z.; Klima, M.; Fudenberg, G.; Hone, J.; Kim, P.; Stormer, H. L. *Solid State Commun.* **2008**, *146*, 351–355.

(4) Balandin, A. A.; Ghosh, S.; Bao, W. Z.; Calizo, I.; Teweldebrhan, D.; Miao, F.; Lau, C. N. *Nano Lett.* **2008**, *8*, 902–907.

(5) Sordan, R.; Traversi, F.; Russo, V. *Appl. Phys. Lett.* **2009**, *94*, 073305.

(6) Lin, Y. M.; Jenkins, K. A.; Valdes-Garcia, A.; Small, J. P.; Farmer, D. B.; Avouris, Ph. *Nano Lett.* **2009**, *9*, 422–426.

(7) Lin, Y.-M.; Dimitrakopoulos, C.; Jenkins, K. A.; Farmer, D. B.; Chiu, H.-Y.; Grill, A.; Avouris, P. *Science* **2010**, *327*, 662–662.

(8) Chen, J. H.; Ishigami, M.; Jang, C.; Hines, D. R.; Fuhrer, M. S.; Williams, E. D. *Adv. Mater.* **2007**, *19*, 3623.

(9) Huang, B.; Li, Z. Y.; Liu, Z. R.; Zhou, G.; Hao, S. G.; Wu, J.; Gu, B. L.; Duan, W. H. *J. Phys. Chem. C* **2008**, *112*, 13442–13446.

(10) Schedin, F.; Geim, A. K.; Morozov, S. V.; Hill, E. W.; Blake, P.; Katsnelson, M. I.; Novoselov, K. S. *Nat. Mater.* **2007**, *6*, 652–655.

(11) Sakhaee-Pour, A.; Ahmadian, M. T.; Vafai, A. *Solid State Commun.* **2008**, *147*, 336–340.

(12) Lu, G. H.; Ocola, L. E.; Chen, J. H. *Nanotechnology* **2009**, *20*, 445–502.

(13) Zhang, Y. P.; Li, H. B.; Pan, L. K.; Lu, T.; Sun, Z. *J. Electroanal. Chem.* **2009**, *634*, 68–71.

(14) Wu, J. B.; Becerril, H. A.; Bao, Z. N.; Liu, Z. F.; Chen, Y. S.; Peumans, P. *Appl. Phys. Lett.* **2008**, *92*, 263302.

(15) Ghosh, S.; Bao, W.; Nika, D. L.; Subrina, S.; Pokatilov, E. P.; Lau, C. N.; Balandin, A. A. *Nat. Mater.* **2010**, *9*, 555–558.

(16) Nair, R. R.; Blake, P.; Grigorenko, A. N.; Novoselov, K. S.; Booth, T. J.; Stauber, T.; Peres, N. M. R.; Geim, A. K. *Science* **2008**, *320*, 1308–1308.

(17) Novoselov, K. S.; Geim, A. K.; Morozov, S. V.; Jiang, D.; Zhang, Y.; Dubonos, S. V.; Grigorieva, I. V.; Firsov, A. A. *Science* **2004**, *306*, 666–9.

(18) Geim, A. K. *Science* **2009**, *324*, 1530–1534.

(19) Hernandez, Y.; Nicolosi, V.; Lotya, M.; Blighe, F. M.; Sun, Z. Y.; De, S.; McGovern, I. T.; Holland, B.; Byrne, M.; Gun'ko, Y. K.; Boland, J. J.; Niraj, P.; Duesberg, G.; Krishnamurthy, S.; Goodhue, R.; Hutchison, J.; Scardaci, V.; Ferrari, A. C.; Coleman, J. N. *Nat. Nanotechnol.* **2008**, *3*, 563–568.

(20) Lotya, M.; Hernandez, Y.; King, P. J.; Smith, R. J.; Nicolosi, V.; Karlsson, L. S.; Blighe, F. M.; De, S.; Wang, Z. M.; McGovern, I. T.; Duesberg, G. S.; Coleman, J. N. *J. Am. Chem. Soc.* **2009**, *131*, 3611–3620.

(21) Hassan, H. M. A.; Abdelsayed, V.; Khder, A. E. R. S.; AbouZeid, K. M.; Terner, J.; El-Shall, M. S.; Al-Resayes, S. I.; El-Azhary, A. A. *J. Mater. Chem.* **2009**, *19*, 3832–3837.

(22) Yang, D.; Velamakanni, A.; Bozoklu, G.; Park, S.; Stoller, M.; Piner, R. D.; Stankovich, S.; Jung, I.; Field, D. A.; Ventrice, C. A.; Ruoff, R. S. *Carbon* **2009**, *47*, 145–152.

(23) Wang, H. L.; Robinson, J. T.; Li, X. L.; Dai, H. J. *J. Am. Chem. Soc.* **2009**, *131*, 9910–9911.

(24) Stankovich, S.; Dikin, D. A.; Dommett, G. H. B.; Kohlhaas, K. M.; Zimney, E. J.; Stach, E. A.; Piner, R. D.; Nguyen, S. T.; Ruoff, R. S. *Nature* **2006**, *442*, 282–286.

(25) Jiao, L. Y.; Zhang, L.; Wang, X. R.; Diankov, G.; Dai, H. J. *Nature* **2009**, *458*, 877–880.

(26) Kosynkin, D. V.; Higginbotham, A. L.; Sinitskii, A.; Lomeda, J. R.; Dimiev, A.; Price, B. K.; Tour, J. M. *Nature* **2009**, *458*, 872–876.

(27) Reina, A.; Thiele, S.; Jia, X.; Bhaviripudi, S.; Dresselhaus, M.; Schaefer, J.; Kong, J. *Nano Res.* **2009**, *2*, 509–516.

(28) Reina, A.; Jia, X. T.; Ho, J.; Nezich, D.; Son, H. B.; Bulovic, V.; Dresselhaus, M. S.; Kong, J. *Nano Lett.* **2009**, *9*, 30–35.

(29) Kim, K. S.; Zhao, Y.; Jang, H.; Lee, S. Y.; Kim, J. M.; Ahn, J. H.; Kim, P.; Choi, J. Y.; Hong, B. H. *Nature* **2009**, *457*, 706–10.

(30) Yu, Q. K.; Lian, J.; Siriponglert, S.; Li, H.; Chen, Y. P.; Pei, S. S. *Appl. Phys. Lett.* **2008**, *93*, 113103.

(31) Chae, S. J.; Gunes, F.; Kim, K. K.; Kim, E. S.; Han, G. H.; Kim, S. M.; Shin, H. J.; Yoon, S. M.; Choi, J. Y.; Park, M. H.; Yang, C. W.; Pribat, D.; Lee, Y. H. *Adv. Mater.* **2009**, *21*, 2328–2333.

(32) Bae, S.; Kim, H.; Lee, Y.; Xu, X.; Park, J.-S.; Zheng, Y.; Balakrishnan, J.; Lei, T.; Ri Kim, H.; Song, Y. I.; Kim, Y.-J.; Kim, K. S.; Ozyilmaz, B.; Ahn, J.-H.; Hong, B. H.; Iijima, S. *Nat. Nanotechnol.* **2010**, *5*, 574–578.

(33) Campos-Delgado, J.; Romo-Herrera, J. M.; Jia, X. T.; Cullen, D. A.; Muramatsu, H.; Kim, Y. A.; Hayashi, T.; Ren, Z. F.; Smith, D. J.; Okuno, Y.; Ohba, T.; Kanoh, H.; Kaneko, K.; Endo, M.; Terrones, H.; Dresselhaus, M. S.; Terrones, M. *Nano Lett.* **2008**, *8*, 2773–2778.

(34) Li, X. S.; Cai, W. W.; An, J. H.; Kim, S.; Nah, J.; Yang, D. X.; Piner, R.; Velamakanni, A.; Jung, I.; Tutuc, E.; Banerjee, S. K.; Colombo, L.; Ruoff, R. S. *Science* **2009**, *324*, 1312–1314.

(35) Coraux, J.; Diaye, A. T.; Busse, C.; Michely, T. *Nano Lett.* **2008**, *8*, 565–570.

(36) Chong-an, D.; Dacheng, W.; Gui, Y.; Yunqi, L.; Yunlong, G.; Daoben, Z. *Adv. Mater.* **2008**, *20*, 3289–3293.

(37) Marchini, S.; Gunther, S.; Wintterlin, J. *Phys. Rev. B* **2007**, *76*, 075429.

(38) Berger, C.; Song, Z.; Li, X.; Wu, X.; Brown, N.; Naud, C.; Mayou, D.; Li, T.; Hass, J.; Marchenkov, A. N.; Conrad, E. H.; First, P. N.; de Heer, W. A. *Science* **2006**, *312*, 1191–1196.

(39) Srivastava, A.; Galande, C.; Ci, L.; Song, L.; Rai, C.; Jariwala, D.; Kelly, K. F.; Ajayan, P. M. *Chem. Mater.* **2010**, *22*, 3457–3461.

(40) Mattevi, C.; Eda, G.; Agnoli, S.; Miller, S.; Mkhoyan, K. A.; Celik, O.; Mostrogiovanni, D.; Granozzi, G.; Garfunkel, E.; Chhowalla, M. *Adv. Funct. Mater.* **2009**, *19*, 2577–2583.

(41) Gomez-Navarro, C.; Meyer, J. C.; Sundaram, R. S.; Chuvilin, A.; Kurasch, S.; Burghard, M.; Kern, K.; Kaiser, U. *Nano Lett.* **2010**, *10*, 1144–1148.

(42) Jiao, L. Y.; Fan, B.; Xian, X. J.; Wu, Z. Y.; Zhang, J.; Liu, Z. F. *J. Am. Chem. Soc.* **2008**, *130*, 12612–12613.

(43) Reina, A.; Son, H. B.; Jiao, L. Y.; Fan, B.; Dresselhaus, M. S.; Liu, Z. F.; Kong, J. *J. Phys. Chem. C* **2008**, *112*, 17741–17744.

(44) Liu, B. L.; Ren, W. C.; Liu, C.; Sun, C. H.; Gao, L. B.; Li, S. S.; Jiang, C. B.; Cheng, H. M. *ACS Nano* **2009**, *3*, 3421–3430.

(45) Liu, B.; Ren, W.; Gao, L.; Li, S.; Pei, S.; Liu, C.; Jiang, C.; Cheng, H.-M. *J. Am. Chem. Soc.* **2009**, *131*, 2082–2083.

(46) Huang, S.; Cai, Q.; Chen, J.; Qian, Y.; Zhang, L. *J. Am. Chem. Soc.* **2009**, *131*, 2094–2095.

(47) Ferrari, A. C.; Meyer, J. C.; Scardaci, V.; Casiraghi, C.; Lazzeri, M.; Mauri, F.; Piscanec, S.; Jiang, D.; Novoselov, K. S.; Roth, S.; Geim, A. K. *Phys. Rev. Lett.* **2006**, *97*, 187401.

(48) Gupta, A.; Chen, G.; Joshi, P.; Tadigadapa, S.; Eklund, P. C. *Nano Lett.* **2006**, *6*, 2667–2673.

(49) Lander, J. J.; Kern, H. E.; Beach, A. L. *J. Appl. Phys.* **1952**, *23*, 1305–1309.

(50) Mclellan, R. B. *Scr. Metall.* **1969**, *3*, 389–392.

(51) Nicholas, N. W.; Connors, L. M.; Ding, F.; Yakobson, B. I.; Schmidt, H. K.; Hauge, R. H. *Nanotechnology* **2009**, *20*, 245607.

(52) Yao, Y.; Feng, C.; Zhang, J.; Liu, Z. *Nano Lett.* **2009**, *9*, 1673–1677.